Journal of Alloys and Compounds 495 (2010) 655–658

Contents lists available at ScienceDirect

Journal of Alloys and Compounds

journal homepage: www.elsevier.com/locate/jallcom

Synthesis of $Mg_{15}Fe$ materials for hydrogen storage applying ball milling procedures

J.A. Puszkiel*, F.C. Gennari, P. Arneodo Larochette

Instituto Balseiro (UNCuyo and CNEA), Consejo Nacional de Investigaciones Científicas y Técnicas, (CONICET) and Centro Atómico Bariloche, Av. Bustillo km 9.5, R8402AGP, S.C. de Bariloche, Argentina

ARTICLE INFO

Article history:
Received 18 July 2008
Received in revised form 19 May 2009
Accepted 3 October 2009
Available online 13 October 2009

Keywords:
Hydrogen storage
Metallic hydrides
Ball milling

ABSTRACT

The effects of different synthesis procedures on the microstructure and hydrogen uptake characteristics of the $Mg_{15}Fe$ materials were studied. The applied processes of synthesis consisted basically on ball milling in argon atmosphere followed by a hydriding reaction. Two mill devices with distinct milling modes were employed, i.e. a low energy mill (LEM) (Magneto Uni-Ball-Mill II) and a high energy mill (HEM) (Fritsch Planetary Mill, P6). The HEM sample showed better Mg–Fe mixing degree than the sample obtained from the LEM process due to the small particles of Fe resulting from the larger amount of mechanical energy transferred to the materials by the HEM device. The better Mg–Fe contacting was responsible for the higher hydrogen capacity and faster hydrogen uptake rate of the high energy milled material. Therefore, the HEM procedure was more effective than the LEM. The hydrogen uptake properties of the HEM synthesized material were compared with other Mg-based materials obtained via inert and reactive ball milling without a subsequent activation step. This study showed that $Mg_{15}Fe$ mixture of powders synthesized via reactive ball milling in hydrogen (RBM–LEM) has higher hydrogen capacity (5.5 wt% H) and faster kinetics than samples with the same composition milled in argon (LEM – 1.65 wt% H and HEM 1.87 wt% H). Nevertheless, a superior hydrogen capacity (6.5 wt% H) were obtained by adding $LiBH_4$ to $Mg_{15}Fe$ via HEM in argon atmosphere.

© 2009 Elsevier B.V. All rights reserved.

1. Introduction

Among all the solid materials studied so far, magnesium provides an attractive option to store hydrogen by virtue of its high hydrogen capacity of 7.6 wt% H, abundance and low cost. However, magnesium hydride presents many disadvantages because of its high thermodynamic stability and slow desorption kinetics, which makes this material not appropriate for practical applications [1]. These constraints can be improved by combining magnesium with a transition metal and the reduction of the particle and crystallite size of the material at nanometer scale [2]. Ball milling procedures are well-known methods for processing metallic powders, able to reduce the particle and crystallite size and mix intimately the combined metallic powders [2–7]. These effects enhance the hydrogen transport properties and can improve the kinetic characteristics of the materials.

In previous works [8,9] we showed that the hydrogen storage properties of Mg can be improved by the addition of Fe in a Mg_2Fe stoichiometric proportion and the application of ball milling (BM) as a method of synthesis. After studying different Mg–Fe compositions synthesized by reactive ball milling (RBM), we then found that a material with a $Mg_{15}Fe$ composition presents better hydrogen storage capacity than the other tested Mg_XFe ($X = 2$ and 3) compositions and good kinetics [10].

In this work, the synthesis of hydride compounds was initially carried out using $Mg_{15}Fe$ and applying ball milling (BM) in an inert atmosphere followed by a hydriding reaction at high temperature and pressure. For this purpose two different milling procedures were employed, viz. low (LEM) and high energy milling (HEM). The main BM parameters were calculated applying developed models [11–14]. Based on the microstructural analysis and the hydrogen uptake properties, it was concluded that the HEM procedure is more effective than the LEM. However, the hydrogen uptake capacity of the HEM samples was low (HEM – 1.87 wt% H at 623 K). In order to improve the H capacity of $Mg_{15}Fe$, the RBM (H_2) was applied and an additive was tried. First, the synthesis by LEM in H_2 atmosphere using $Mg_{15}Fe$ as initial material was applied. RBM was employed because it is an in-situ synthesis method through which a high degree of microstructural refinement can be reached due to the further grain size reduction of Mg embrittled by H_2. Then, it was tried the addition of $LiBH_4$ to $Mg_{15}Fe$ applying HEM in argon. $LiBH_4$ has high hydrogen capacity (18.4 wt% H), but unfortunately it is very stable and decomposes above 673 K. The addition of $LiBH_4$ to

* Corresponding author.
E-mail addresses: jpuszkiel@cab.cnea.gov.ar (J.A. Puszkiel), gennari@cab.cnea.gov.ar (F.C. Gennari), arneodo@cab.cnea.gov.ar (P.A. Larochette).

0925-8388/$ – see front matter © 2009 Elsevier B.V. All rights reserved.
doi:10.1016/j.jallcom.2009.10.011

$Mg_{15}Fe$ is based on superior hydrogen storage properties achieved when Mg is combined with $LiBH_4$ [15–17]

2. Experimental

Stoichiometric $Mg_{15}Fe$ mixtures of powders (5–10 g) were subjected to two different BM procedures. The first was LEM in a Magneto-mill Uni-Ball-Mill II (Australian Scientific Instruments) at 180 rpm (vial speed) during 150 h using vials and balls (25.4 mm of diameter) of stainless steel. The second was HEM in a planetary mill (Pulverisette P6) at 360 rpm (disc speed) during 30 h using vials and balls (16.5 mm of diameter) of stainless steel. Both BM processes were carried out in argon gas (0.1 MPa, purity >99.9995%), at room temperature and maintaining the same ball to powder ratio of 40:1. The determination of the LEM duration was based on previous studies carried out with the same materials [8–10]. On the other hand, the HEM duration was established taking into account no further reduction of the grain size of the elemental powders. These two milling processes were applied in order to compare the microstructural characteristics and the effects on the hydrogen storage properties of the resulting materials.

During the BM processes the vial was opened several times in order to take samples for analysis. The microstructural evolution of the materials during milling was investigated by XRD patterns (Philips PW 1710/01 Instruments) using CuKα radiation (λ = 1.5405 Å, graphite monochromator, 30 mA and 40 kV). Scherrer equation was applied to calculate the crystallite size of Mg and Fe. Morphological and chemical analyses of the samples were performed by scanning electron microscopy (SEM 515, Philips Electronic Instruments) equipped with EDS microanalysis. Backscattered electron micrographs were taken on resin mounted and polished samples. The values of Fe and Mg atomic percentages of the as-milled powders were estimated by EDS as an average of seven measurements, two taken from general sectors of the resin mounted and polished samples and five taken from different sectors of powders dispersed on a stick. The particle size distributions of the starting materials and as-milled powders were estimated using Mastersizer Micro MAF 5000. All handlings were done in a glove box with argon gas, with oxygen and moisture controlled atmosphere (<1 ppm), so as to minimize the degradation of the samples.

After milling, a hydriding reaction (activation) of the as-milled powders was performed at 673 K and 6 MPa. The activation of the materials and the evaluation of the hydrogen storage uptake properties of the as-milled materials were carried out in a Sieverts-type device [18]. Measurements of the hydrogen absorption rates and capacities were carried out in the temperature range of 523–673 K. In order to evaluate the effects of the temperature on the hydrogen uptake, all the measurements were performed at the same established relationship between the initial pressure at which the absorption process starts and the equilibrium pressure ($P_i/P_{equilibrium}$ = 2.4) [10].

The hydrogen uptake properties of the $Mg_{15}Fe$ materials synthesized via HEM and LEM in argon atmosphere were also compared with $Mg_{15}Fe$ and $Mg_{15}Fe + LiBH_4$ materials obtained by RBM and BM, respectively. These additional samples were synthesized to improve the hydrogen uptake characteristics of $Mg_{15}Fe$, mainly the hydrogen capacity which was very low for the HEM and LEM samples. One of the samples used for comparison was obtained via LEM in H_2 atmosphere (0.5 MPa, purity >99.999%) during 150 h employing the same ball to powder ratio (40:1), temperature and vial speed used for LEM in inert atmosphere. The other consisted of a $Mg_{15}Fe$ and $LiBH_4$ (~10 wt%) mixture (Sigma Aldrich, purity >90%) obtained by HEM in inert atmosphere. The milling conditions were the same as used for the HEM processes carried out with $Mg_{15}Fe$ mixture of powders, but the time required to achieve a good degree of microstructural requirement was 15 h. These samples did not require the activation step.

3. Results and discussion

3.1. Theoretical models: ball milling parameters

Whilst the main milling mode for LEM is impact (caused by gravity and magnetic forces), for HEM the main milling mechanism is friction. Hence, different models were applied to estimate the milling parameters. In the case of LEM, the milling parameters were estimated applying a model developed in Ref. [11]. On the other hand, the milling parameters for HEM were calculated employing a model for planetary mills [12–14] and taking into account the characteristics of the utilized mill (Pulverisette P6). According to previous works [12,13], the reached microstructural refinement of the powders subjected to milling procedures depends mainly on the injected shock power (P) or injected shock power per unit mass of grinding medium (P_g) and the total transferred energy (E_T), given by the following equations:

$$P\ (\mathrm{W}) = f\,E_K \tag{1}$$

$$P_g\,(\mathrm{W/g}) = \frac{P}{m_b} \tag{2}$$

$$E_T\,(\mathrm{J}) = \mathrm{BMD}\,P\,Nb \tag{3}$$

where f(Hz): shock frequency of one ball, E_K (J): kinetic energy, m_b (g): mass of grinding medium. BMD (s): ball milling duration, Nb: Number of balls used as grinding medium.

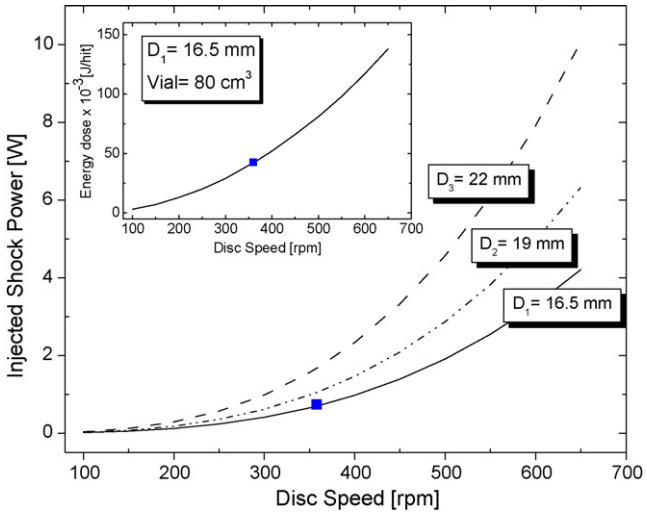

Fig. 1. Injected shock power (W) as a function of the disc speed (rpm) and diameters (mm) of the grinding medium (stainless steel balls of different diameters (D) and mass (m): D_1 = 16.5 mm and m_1 = 18.9 g; D_2 = 19 mm and m_2 = 28.3 g; D_3 = 22 mm and m_3 = 45 g) for a vial of 80 cm^3. Inset plot: Energy dose (10^{-3} J/hit) as a function of the disc speed (rpm) for the used HEM milling conditions. The squared points indicate the disc speed and energy parameters at which the HEM procedure was carried out.

In Table 1 are reported the main parameters of different mill devices and the milling conditions at which the milling procedures were performed in this work (values in parentheses). The P_g achieved with the HEM (P_g = 0.04 W/g) is larger than the LEM (P_g = 0.0003 W/g). Moreover, a 10 times higher E_T is reached with the HEM in a shorter time (30 h). These results show that the HEM was more efficient than the LEM since the former transferred more mechanical energy to the powders than the latter. The curves of the injected shock power, P (W), and energy dose, E_D (10^{-3} J/hit), versus the disc speed (rpm) for the planetary mill device (HEM) are shown in Fig. 1. As can be seen, P increases with the disc speed and the diameter (mass) of the grinding medium. Considering the used disc speed and grinding medium, the

Table 1
Documented [13] and in this work calculated ball milling parameters of different mill devices. The values in parentheses correspond to the milling conditions used in this work. Parameters: V_b: impact speed of one ball; E_D: Energy dose defined as kinetic energy released from one ball to the powders in one hit; f: shock frequency of one ball; P_g: injected shock power per unit mass of grinding medium.

Mill	V_b (m/s)	E_D (10^{-3} J/hit)	f (Hz)	P_g (W/g)
Pulv. 5 [8]	2.5–4	10–400	~40	0.01–0.8
G7 [8]	0.24–6.58	0.4–303	5–92	0–0.56
G5 [8]	0.28–11.24	0.53–884	4.5–90	0–1.6
Magneto Uni-Ball-Mill [11]	0–2 (1.5)	50–140 (140)	0.16–2.7 (0.16)	0.0003–0.002 (0.0003)
Fritsch Pulv. 6 [This work]	0.6–3.8 (2.1)	3–138 (42)	4.7–30 (17)	0.001–0.22 (0.04)

Table 2
Crystallite size of Mg (1 0 1) and Fe (1 1 0), relative atomic percentages (EDS) and agglomerate size distributions (D) of the initial and the as-milled (LEM and HEM) materials.

	Grain size (nm)	EDS (at%)	D [v, 0.1][a] (μm)	Volume mean diameter (μm)	D [v, 0.9][b] (μm)
Initial materials					
Mg	45	–	131	198	263
Fe	40	–	43	85	137
LEM (150 h)					
Mg	30	95	55	92	134
Fe	20	5			
HEM (30 h)					
Mg	35	95	52	113	192
Fe	25	5			

[a] 10% of the volume distribution (v) is below this value.
[b] 90% of the volume distribution (v) is below this value.

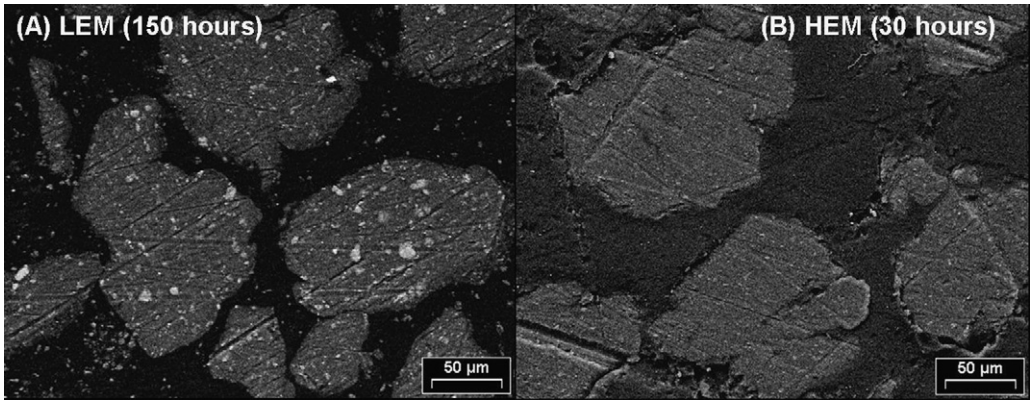

Fig. 2. Backscattered electron micrographs of (A) the low energy milled materials and (B) the high energy milled materials.

squared point indicates the HEM energy conditions reached in this work.

3.2. Ball milling procedures

The characteristics of the initial and as-milled materials are shown in Table 2. The crystallite sizes of Mg and Fe (XRD patterns not shown) have been reduced from 45 to ~30 nm and from 40 to ~20 nm, respectively. In relation to the starting materials the final agglomerate size distribution was not considerably modified. It is also noticed that the crystallite size, agglomerate size and distribution of the as-milled powders are similar. Moreover, several EDS analyses show that the atomic percentages of Fe and Mg in the samples after milling are practically the same. These values are very close to the theoretical composition, viz. 93 at% of Mg and 7 at% of Fe. Fig. 2 shows backscattered electron micrographs of the as-milled materials. The Fe particles (bright phase) are embedded in the Mg matrix (dark phase) which acts as the ductile phase. Clearly, the particles of Fe are smaller in the HEM sample (Fig. 2B), ~2 μm, than those found in the LEM sample (Fig. 2A), ~10 μm.

Based on the results shown in Table 2, the LEM and HEM samples do not present significant differences concerning the degree of microstructural refinement, Mg and Fe atomic percentages and agglomerate size and distribution. However, the backscattered electron micrographs (Fig. 2) show that the HEM process further reduces the particles of Fe making possible a better Mg–Fe mixing degree and contacting. This is a direct consequence of the larger amount of mechanical energy imparted to the material by the HEM.

3.3. Hydriding reaction: activation

For activation, the as-milled $Mg_{15}Fe$ powders (HEM and LEM) were subjected to a hydriding reaction at 673 K and 6 MPa during 15 h. The weight percentages of the phases and total hydrogen uptake are shown in Table 3. These weight percentages were calculated from the stoichiometric proportions of the starting materials and the amounts of hydride phases, i.e. MgH_2 and Mg_2FeH_6, obtained from a desorption isotherm carried out at 673 K after the activation process.

3.4. Hydrogen uptake properties

The hydrogen absorption behavior of the $Mg_{15}Fe$ synthesized samples was measured in the range of temperatures from 523 to 673 K. Considering that the Mg_2FeH_6–MgH_2 hydride system presents one flat plateau during the absorption process in equilibrium conditions and the dependence of the kinetic behavior on the equilibrium pressure, we performed all the kinetic measurements at a settled relationship between the initial pressure and the equilibrium pressure ($P_i/P_{equilibrium} = 2.4$) [10]. Fig. 3 shows a clear increase of both the absorption rate and the hydrogen storage capacity with the temperature. At temperatures below 623 K the HEM sample has higher hydrogen capacity and faster hydrogen uptake rate than the LEM sample. This is attributed to the better contacting and mixing degree between Fe and Mg achieved via the HEM procedure (see Fig. 2). On the contrary, at 673 K the HEM sample exhibits slower hydrogen uptake rates than the LEM sample. This effect is ascribed to the formation of a larger amount

Table 3
Relative amount of phases and total hydrogen uptake after the hydriding reaction (activation).

Sample	Mg (wt%)	Fe (wt%)	MgH_2 (wt%)	Mg_2FeH_6 (wt%)	H (wt%)
LEM	34	9	50	7	4.2
HEM	24	7	59	10	5.1

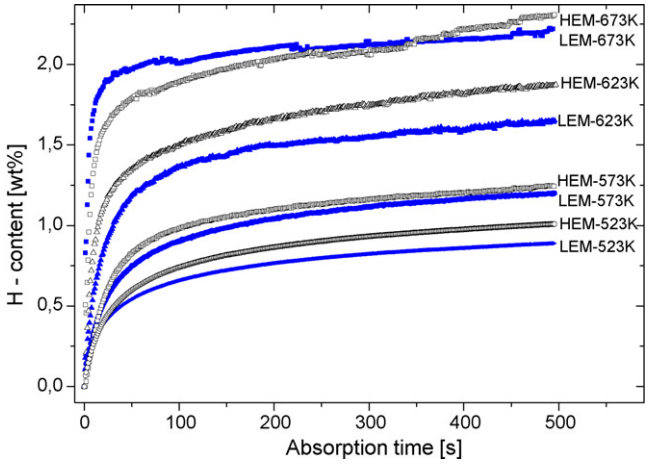

Fig. 3. Hydrogen uptake behavior of the HEM and LEM samples in the temperature range of 523–673 K at a constant relationship between the initial and equilibrium pressures of 2.4.

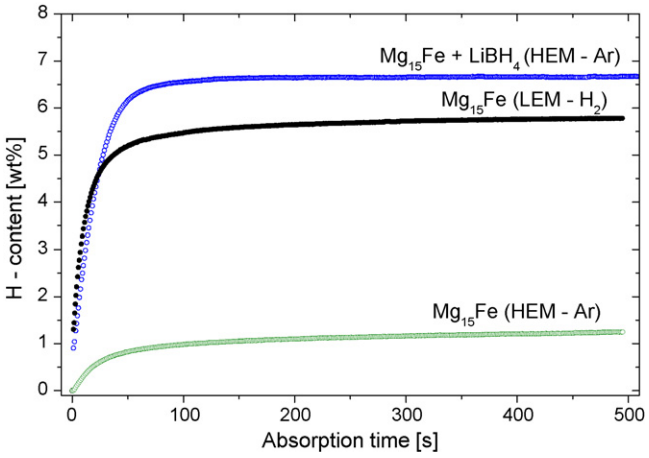

Fig. 4. Hydrogen uptake behavior of $Mg_{15}Fe$ samples synthesized via HEM (Ar) and LEM (H_2), and $Mg_{15}Fe + LiBH_4$ produced via HEM (Ar) at 623 K and a constant relationship between the initial and equilibrium pressures of 2.4.

of Mg_2FeH_6 phase in the HEM (see Table 3), which is a slow process due to the diffusion mechanisms. The same behavior has been already observed in Mg_2Fe samples [9]. Furthermore, the hydrogen capacity of the synthesized materials is lower than its theoretical capacity one (6.6 wt% H – referred to MgH_2). This is in agreement with the unreacted Mg (see Table 3) found in the sample after hydrogen cycling and detected in the XRD patterns (not shown) of the samples taken at 623 K. This fact is attributed to the low degree of microstructural refinement and the poor dispersion of Fe on Mg reached through the milling processes.

Due to the low capacity reached with the LEM and HEM samples, the synthesis of $Mg_{15}Fe$ via LEM in hydrogen atmosphere (RBM) and the addition of $LiBH_4$ to $Mg_{15}Fe$ through HEM in argon atmosphere were tried. Fig. 4 shows the uptake kinetics of $Mg_{15}Fe$ and $Mg_{15}Fe + LiBH_4$ both synthesized via HEM in argon atmosphere and $Mg_{15}Fe$ obtained via RBM. Applying RBM the hydrogen storage uptake characteristics of the $Mg_{15}Fe$ material can be markedly improved due to the high degree of microstructural refinement reached through the hydrogen embrittlement of Mg during the milling process [10,19]. However, by the proper combination of $Mg_{15}Fe$ composition with a small quantity (~10 wt%) of $LiBH_4$ it is possible to produce materials with relative high hydrogen storage capacity (6.5 wt% H) and fast absorption kinetics applying BM in inert atmosphere avoiding the activation step. The addition of $LiBH_4$ to $Mg_{15}Fe$ during the milling process causes an additional Mg agglomerate and crystallite size reduction introducing more defects that serve as diffusion channels for the hydrogen absorption [20].

4. Conclusions

The synthesis of $Mg_{15}Fe$ materials applying HEM in inert atmosphere was more efficient than the LEM, since a material with better hydrogen uptake characteristics was obtained in shorter milling times. On the other hand, $Mg_{15}Fe$ materials produced via LEM in hydrogen atmosphere showed higher hydrogen storage capacity (5.5 wt% H) and faster absorption kinetics than the material with the same composition obtained via HEM in inert atmosphere (1.87 wt% H). Nevertheless, with the addition of $LiBH_4$, it is possible to obtain Mg-based hydride components with larger hydrogen capacity (6.5 wt% H) and good kinetics via HEM in inert atmosphere without the subsequent activation step. Moreover, the synthesis of this sort of hydride mixtures presents two considerable advantages. First, the synthesis via BM in inert atmosphere is easier to control and safer than the RBM. Second, a subsequent activation step of the as-milled materials is not required. Although the synthesis of these hydride mixtures requires further development and its hydrogen storage characteristics must be improved for a potential application, the mentioned advantages are quite important from the large scale production point of view.

Acknowledgments

The authors thank CONICET, ANPCyT and the Instituto Balseiro (UNCuyo) for partial financial support to carry out this work.

References

[1] B. Bogdanović, K. Bohmhamme, B. Christ, A. Reiser, K. Schlichte, R. Vehlen, J. Alloys Compd. 282 (1999) 84–92.
[2] A. Zaluska, L. Zaluski, J.O. Ström-Olsen, J. Alloys Compd. 288 (1999) 217–225.
[3] J. Huot, G. Liang, S. Boily, A. Van Neste, R. Schulz, J. Alloys Compd. 495 (1999) 293–295.
[4] F.C. Gennari, F.J. Castro, G. Urretavizcaya, J. Alloys Compd. 321 (2001) 46–53.
[5] J. Huot, M.L. Tremblay, R. Schulz, J. Alloys Compd. 603 (2003) 356–357.
[6] J.L. Bobet, S. Desmoulins-Krawiec, E. Grigorova, R. Cansell, B. Chevalier, J. Alloys Compd. 351 (2003) 217–221.
[7] A. Bassetti, E. Bonetti, L. Pasquini, A. Montone, J. Grbovic, M. Vittori Antisari, Eur. Phys. J. B43 (2005) 19–27.
[8] J.A. Puszkiel, P. Arneodo Larochette, F.C. Gennari, J. Alloys Compd. 463 (2008) 134–142.
[9] J.A. Puszkiel, P. Arneodo Larochette, F.C. Gennari, Int. J. Hydrogen Energy 33 (2008) 3555–3560.
[10] J.A. Puszkiel, P. Arneodo Larochette, F.C. Gennari, J. Power Sources 186 (2009) 185–193.
[11] J.P. Coutsiers, Summer School, Effects of the different milling parameters in a ball rotator mill, Instituto Balseiro (UNCuyo – CNEA), Centro Atómico Bariloche, 2002. (in Spanish).
[12] M. Abdellaoui, E. Gaffet, J. de Physique IV 4 (1994) 291–296.
[13] M. Abdellaoui, E. Gaffet, J. Alloys Compd. 209 (1994) 351–361.
[14] N. Burgio, A. Iasonna, M. Magini, S. Martelli, F. Padella, Nuovo Cimento 13 (1991) 459.
[15] Y. Nakamori, S. Orimo, J. Alloys Compd. 370 (2004) 271–275.
[16] S.R. Johnson, P.A. Anderson, P.P. Edwards, et al., Chem. Commun. 22 (2005) 2823–2825.
[17] J.F. Mao, et al., J. Phys. Chem. C 111 (2007) 12495–12498.
[18] G. Meyer, D.S. Rodríguez, F. Castro, G. Fernández, Proceedings of the 11th World Energy Conference, Stuttgart, Germany. 23–29 June 1996, 1996, pp. 1293–1298.
[19] J.L. Bobet, B. Chevalier, M.Y. Song, B. Darriet, J. Etourmeau, J. Alloys Compd. 336 (2002) 292–296.
[20] J.A. Puszkiel, F.C. Gennari, Scripta Mater. 60 (2009) 667–670.